



Titre: Can hydrothermal carbonization be used as a mean to increase the circularity of existing food waste anaerobic digestion plants?
Title: Supplément

Auteurs: Fabrice Tanguay-Rioux, Kassem Ibrahim Al Houssaini, Guillaume Majeau-Bettez, Robert Legros, & Laurent Spreutels
Authors:

Date: 2026

Type: Article de revue / Article

Référence: Tanguay-Rioux, F., Al Houssaini, K. I., Majeau-Bettez, G., Legros, R., & Spreutels, L. (2026). Can hydrothermal carbonization be used as a mean to increase the circularity of existing food waste anaerobic digestion plants? Waste Management, 221, 11564 (12 pages). <https://doi.org/10.1016/j.wasman.2026.115624>
Citation:

 **Document en libre accès dans PolyPublie**
Open Access document in PolyPublie

URL de PolyPublie: <https://publications.polymtl.ca/77038/>
PolyPublie URL:

Version: Matériel supplémentaire / Supplementary material
Révisé par les pairs / Refereed

Conditions d'utilisation: Creative Commons Attribution 4.0 International (CC BY)
Terms of Use:

 **Document publié chez l'éditeur officiel**
Document issued by the official publisher

Titre de la revue: Waste Management (vol. 221)
Journal Title:

Maison d'édition: Elsevier
Publisher:

URL officiel: <https://doi.org/10.1016/j.wasman.2026.115624>
Official URL:

Mention légale: © 2026 Published by Elsevier Ltd. This is an open access article under the CC BY license
Legal notice: (<http://creativecommons.org/licenses/by/4.0/>).

Can hydrothermal carbonization be used as a mean to increase the circularity of existing food waste anaerobic digestion plants?

Supplementary information

S1. Pictures of the feedstocks

Pictures of the food waste, the light and heavy rejects and the digestate of both AD plants.



Figure S1: Pictures of the samples from AD plant 1. a) Light rejects (LR1); b) Heavy rejects (HR1); c) Digestate (D1); d) Food waste (FW1).



Figure S2: Pictures of the samples from AD plant 2. a) Light rejects (LR2); b) Heavy rejects (HR2); c) Digestate (D2); d) Food waste (FW2).

S2. Pictures of the hydrochars

Pictures of the hydrochars produced from the different samples after separation and drying.



Figure S3: Pictures of the hydrochars from AD plant 1. a) Light rejects (H-LR1); b) Digestate (H-D1); c) Food waste (H-FW1).



Figure S4: Pictures of the hydrochars from AD plant 2. a) Light rejects (H-LR2); b) Heavy rejects (H-HR2); c) Digestate (H-D2); d) Food waste (H-FW2).

S3. Characterization of the ash

Table S1. Complete results for the XRF analysis

	Al (%)	Ca (%)	Fe (%)	K (%)	Mg (%)	Mn (%)	Na (%)	P (%)	Si (%)	S (%)	Ti (% of ash)	Sr (ppm)	Zn (ppm)	Cr (ppm)	Zr (ppm)	Ni (ppm)	Cu (ppm)
FW1	1.03	17.60	0.75	3.99	0.68	0.02	13.24	4.16	4.47	0.59	0.12	270.8	538.4	<31	42.6	39.6	557.2
LR1	1.07	32.71	0.56	3.48	0.82	<0.007	1.63	0.70	4.26	0.35	0.10	900.9	213.4	<31	77.7	12.4	153.2
D1	4.73	10.47	6.90	2.93	1.38	0.09	1.70	2.87	19.43	0.84	0.28	416.8	536.1	116.8	155.7	44.2	173.3
FW2	5.81	13.78	19.94	3.70	0.90	0.09	2.09	7.04	9.62	4.22	0.21	85.4	2651.2	312.2	<18	100.1	1279.4
LR2	2.57	16.47	6.99	7.22	1.27	0.09	3.62	3.40	11.90	1.85	0.17	514.1	1131.6	113.0	79.0	46.5	538.2
HR2	1.02	33.38	1.35	0.96	0.62	0.02	0.75	2.56	4.26	0.27	0.04	427.7	568.0	127.9	43.1	51.1	103.8
D2	3.70	14.78	13.74	5.43	1.19	0.02	3.23	5.54	9.04	2.68	0.14	266.0	1362.0	182.0	70.3	235.2	699.6
H-FW1	2.83	20.62	2.15	3.29	0.97	0.01	9.60	4.24	8.87	1.32	0.19	329.1	1320.0	313.7	80.3	338.6	665.7
H-LR1	1.82	28.04	1.87	1.31	1.16	0.03	0.74	8.60	7.68	0.63	1.26	341.8	684.9	126.3	80.5	80.6	281.9
H-D1	4.85	12.01	7.35	1.68	1.41	0.10	1.33	3.09	18.98	0.68	0.27	447.6	584.3	138.9	144.8	63.1	201.8
H-FW2	2.82	13.50	21.31	1.75	0.66	0.15	1.12	7.34	6.69	3.70	0.20	363.6	2795.2	271.8	62.9	247.1	1152.3
H-LR2	4.62	15.54	9.13	3.04	1.52	0.14	1.97	5.17	15.97	2.19	0.55	327.0	1619.7	282.9	71.3	602.5	1270.7
H-HR2	0.57	35.71	1.01	0.17	0.53	0.02	0.35	8.80	1.89	0.14	0.03	415.8	1254.3	42.7	27.5	16.4	60.8
H-D2	3.46	15.77	13.83	1.88	0.80	0.07	1.03	6.46	9.83	2.84	0.19	403.9	2256.4	202.7	71.6	152.4	912.7

S4. Energy balance

Method

The higher heating value (HHV) of the hydrochar was estimated with the regression equation developed by Marzban et al. (2022) for char produced under similar conditions (Eq.).

$$HHV_{hyd} = 0.3853C + \frac{44.98}{O} \quad (\text{Eq.S1})$$

Where HHV_{hyd} is the HHV of the hydrochar in MJ kg^{-1} , C is the carbon content in the hydrochar (%) and O is the oxygen concentration in the hydrochar (%).

For the energy balance, it was assumed that the additional energy needed to operate the HTC corresponds only to the energy required to heat the content of the reactor to its operating temperature. Therefore, the heat losses are considered to be negligible in comparison to the heating phase. Since the reactions occur at high temperature, the PW exiting the HTC reactor needs to be cooled down to a temperature close to $35\text{ }^{\circ}\text{C}$ before entering the AD reactor. This energy could be recovered with a heat exchanger to heat the anaerobic digester or pre-heat the feedstock. The additional energy consumption is therefore expressed as:

$$Q_{in} = Q_{HTC} = \frac{m_f}{TS} C_p \Delta T (1 - \eta_{rec}) \quad (\text{Eq.S2})$$

Where Q_{in} is the energy needed for the process (kJ), Q_{HTC} is the energy needed for the HTC step (kJ), m_f is the mass of feedstock on a dry basis (kg), TS is the total solids content of the feedstock (kg kg^{-1}), C_p is the specific heat capacity of the feedstock ($\text{kJ kg}^{-1} \text{K}^{-1}$), ΔT is the temperature difference (K) and η_{rec} is the energy recovery efficiency.

For the calculation, the specific heat capacity (C_p) of the feedstock was assumed to be the same as that of water. An energy recovery efficiency from the HTC slurry (mix of hydrochar and PW) of 0.6 was also assumed based on previous work on the LCA of the HTC of FW (Mayer et al., 2021). In that work, Mayer et al. (2021) calculated that the energy recovered from the HTC slurry for preheating purposes corresponded to about 60% of the total energy consumption (heat loss and heat demand). It was also assumed that the

feedstock enters the system at 20 °C and the HTC is operated at 180 °C. Finally, the feedstock is considered to be diluted with water to a moisture content of 80%, except for FW2 and D2, for which no dilution is required.

The potential energy that could be generated from converting the PW into biogas is determined using the following equation:

$$Q_B = BMP_f m_f HHV_{CH_4} \quad (\text{Eq.S3})$$

where Q_B is the energy production that could be obtained from the biogas (kJ), HHV_{CH_4} is the higher heating value of CH_4 (39.8 kJ L⁻¹), m_f is the mass of feedstock on a dry basis (kg) and the BMP is expressed on a dry feedstock basis (L CH_4 kg⁻¹ TS).

Results

The HTC valorization of the rejects and digestate streams can lead to the production of a significant quantity of additional CH_4 . To be viable, the process should however consume less energy than it produces. Moreover, this net positive energy balance should be valid when considering only the additional CH_4 production, as the final utilization of the hydrochar remains uncertain. The hydrochar produced from HR and D have a high ash content, and all hydrochars have low FC content, which might limit their utilization for energy production. Therefore, the energy needed to convert the different sampled AD streams (Q_{in}) by HTC was compared to the additional energy that could be recovered under the form of biogas (Q_B) through PW recirculation into the digester.

Results of the energy balance are presented in Figure S5. These results consider that the PW would be converted in the same anaerobic digester and that no additional energy is needed related to the conversion of the PW into the digester. The separation of the hydrochar was also not considered as it was considered to be negligible. Finally, it is well known that the actual methane production of a digester is lower than the BMP. The value presented here is thus an overestimation of the amount of methane that would really be produced. Still, it provides an overview of the energy balance of the process.

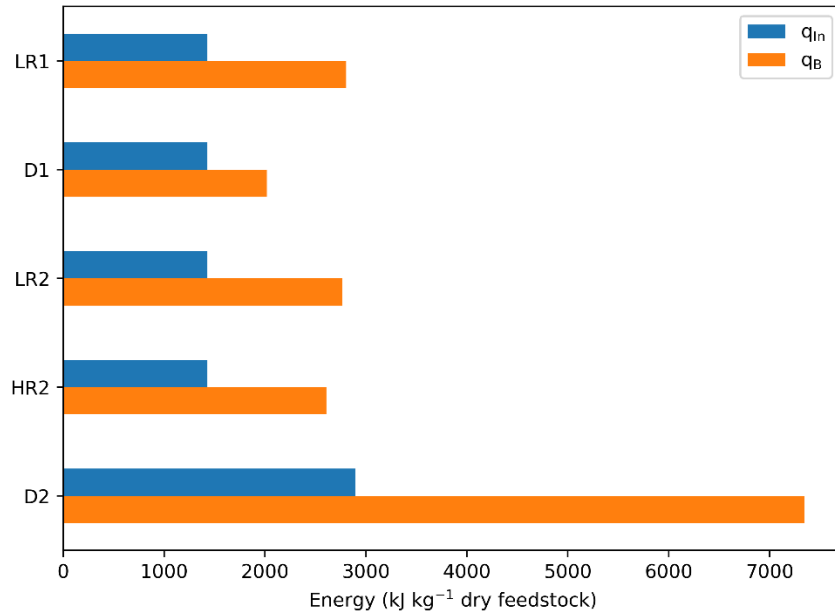


Figure S5: Comparison of the energy requirement and the energy production as biogas by the HTC of the different AD streams expressed per kg of dry feedstock.

For all the cases considered, more energy is produced by the combined HTC-AD process for the conversion of the LR, the HR and the D streams. Therefore, the additional methane generated from the PW following the HTC of reject and digestate streams compensates for the additional energy required to convert these streams. This is valid even if the hydrochar is not used for energy production. The energy balance could thus be even more positive in the cases for which the hydrochar would have a quality suitable for energy valorization.

Since only one sample per stream and per plant was collected and tested, comparisons between them are subject to considerable uncertainty associated with the measurements and the heterogeneity of the materials. Nevertheless, despite the differences in PW compositions and BMPs, all results led to a positive energy balance, indicating that the normal variation of feedstocks should not lead to major differences in the energy balance.

Therefore, despite their differences, both reject streams (LR and HR) could be partially converted into additional CH₄, while also reducing the cost associated with disposal of these fractions. This could represent

an interesting opportunity to increase the circularity of AD facilities. As for converting the digestate, it could represent an interesting additional production of energy. It should however be compared to a direct soil application to validate the environmental benefits achieved.

S5. System boundaries for the Life-Cycle Assessment

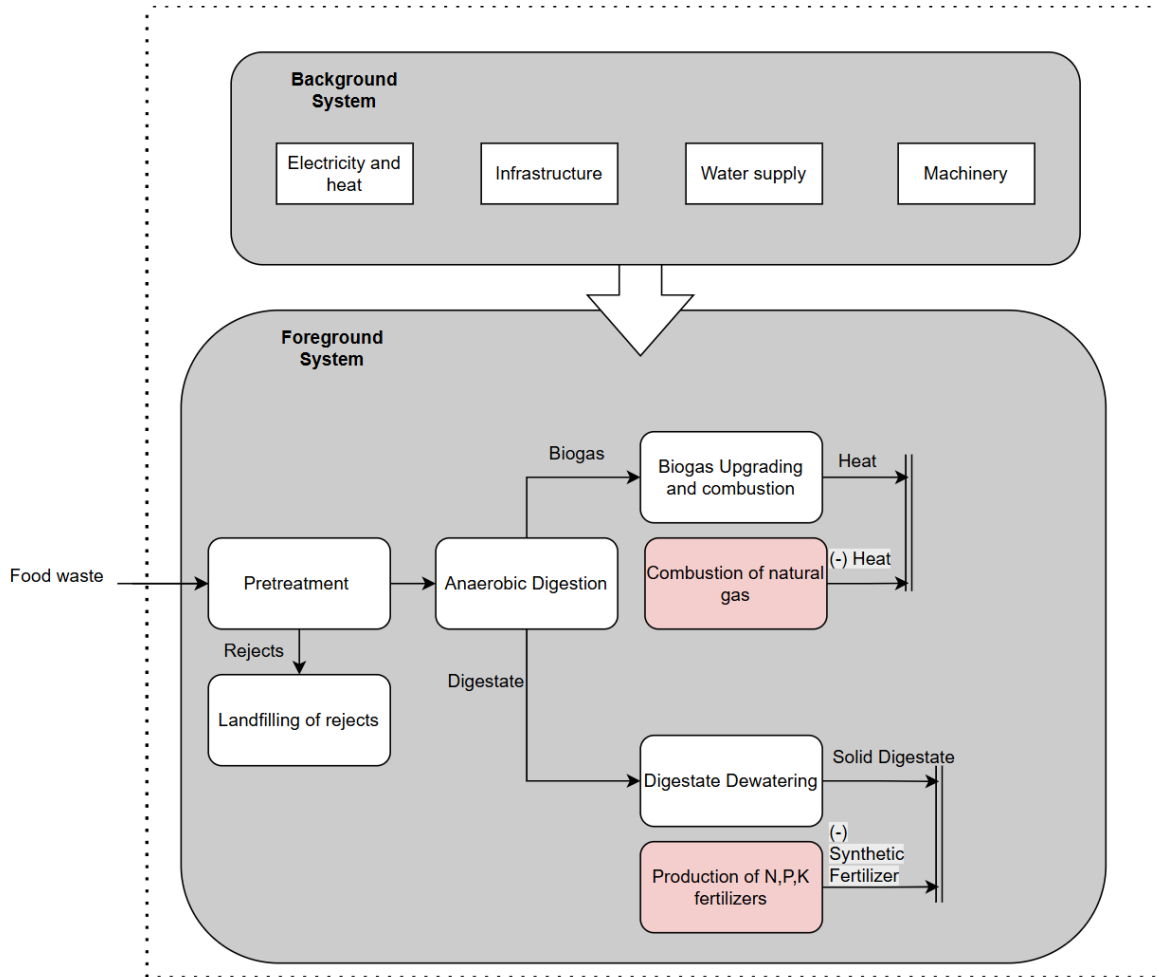


Figure S6: Simplified system boundaries of baseline configurations.

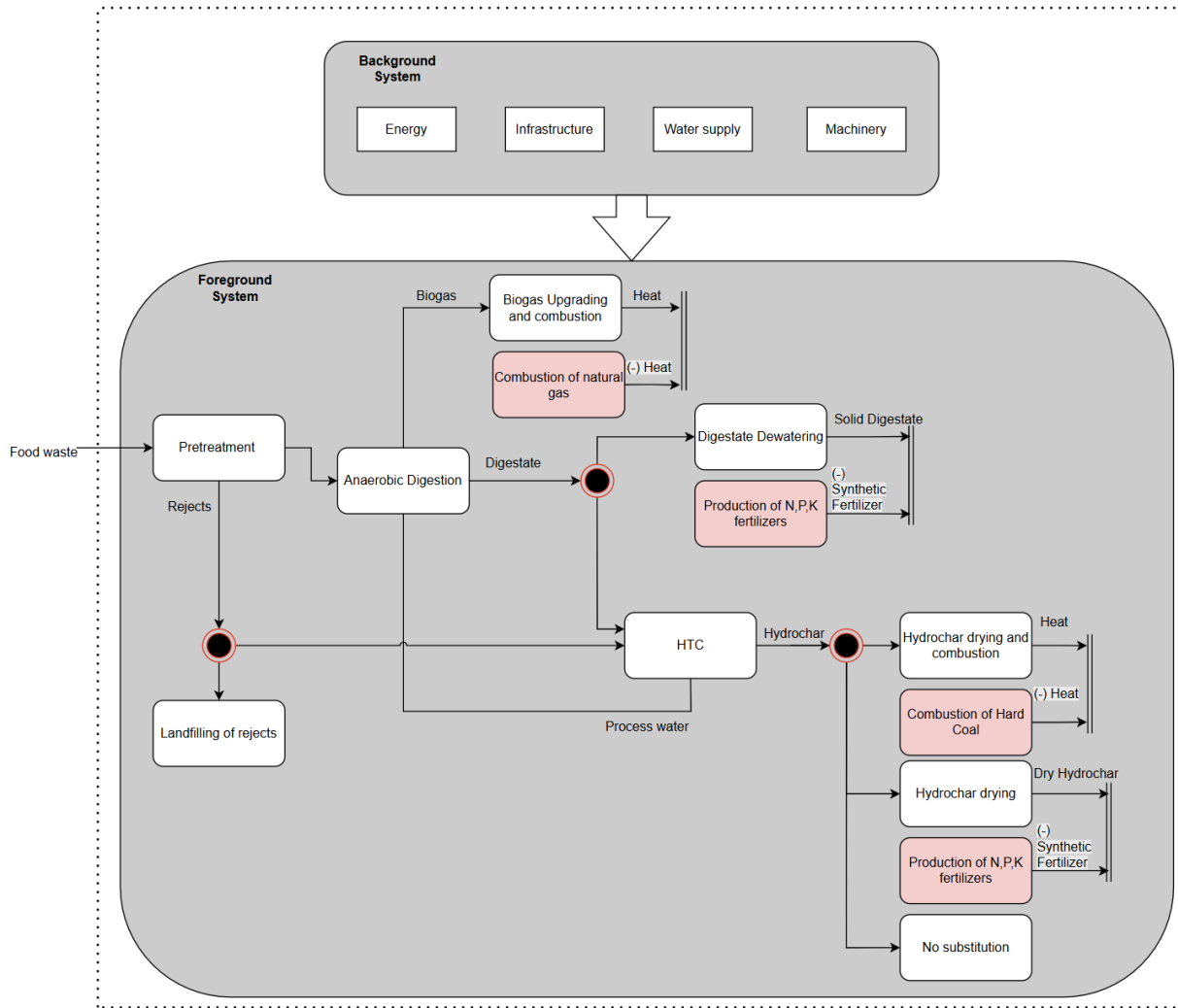


Figure S7: Simplified system boundaries of AD-HTC configurations.

For the system boundaries of the HTC of digesterate from plant 1, D1-HC was dried before entering HTC (only exception to diagram above).

S6. Impacts on Ecosystem Quality and Human Health for the LCA

Fig S8 shows the total ecosystem quality impacts (PDF·m²·yr) for the 17 configurations using the IW+ impact assessment method. The results are consistent with the LCA discussion, confirming that hydrochar use as a solid fuel substitute is the most favorable option and that nearly all pathways perform as well as or better than the baseline (particularly better for the rejects), indicating no burden shifting in this category. For clarity, technologies contributing less than 15% of the total positive impacts are grouped under “Others”.

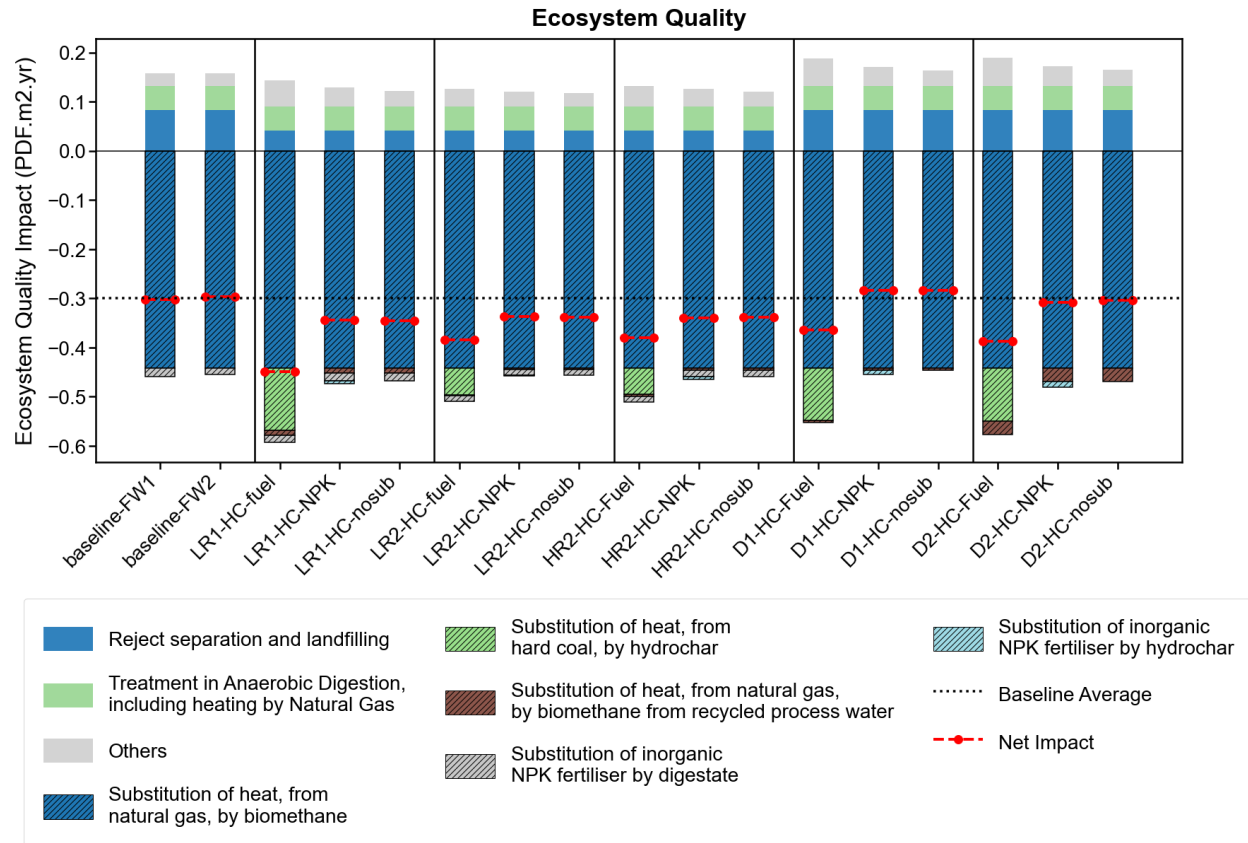


Figure S8: LCA results on the Total Ecosystem Quality (EQ) impact category for the 17 process configurations.

For the Human Health impact category (DALY), no burden shifting is observed, and the same conclusions as for ecosystem quality apply. As with EQ, contributions representing less than 15% of the total positive

impacts are grouped under “Others.” In this category, natural gas heating for AD emerges as the main hotspot.

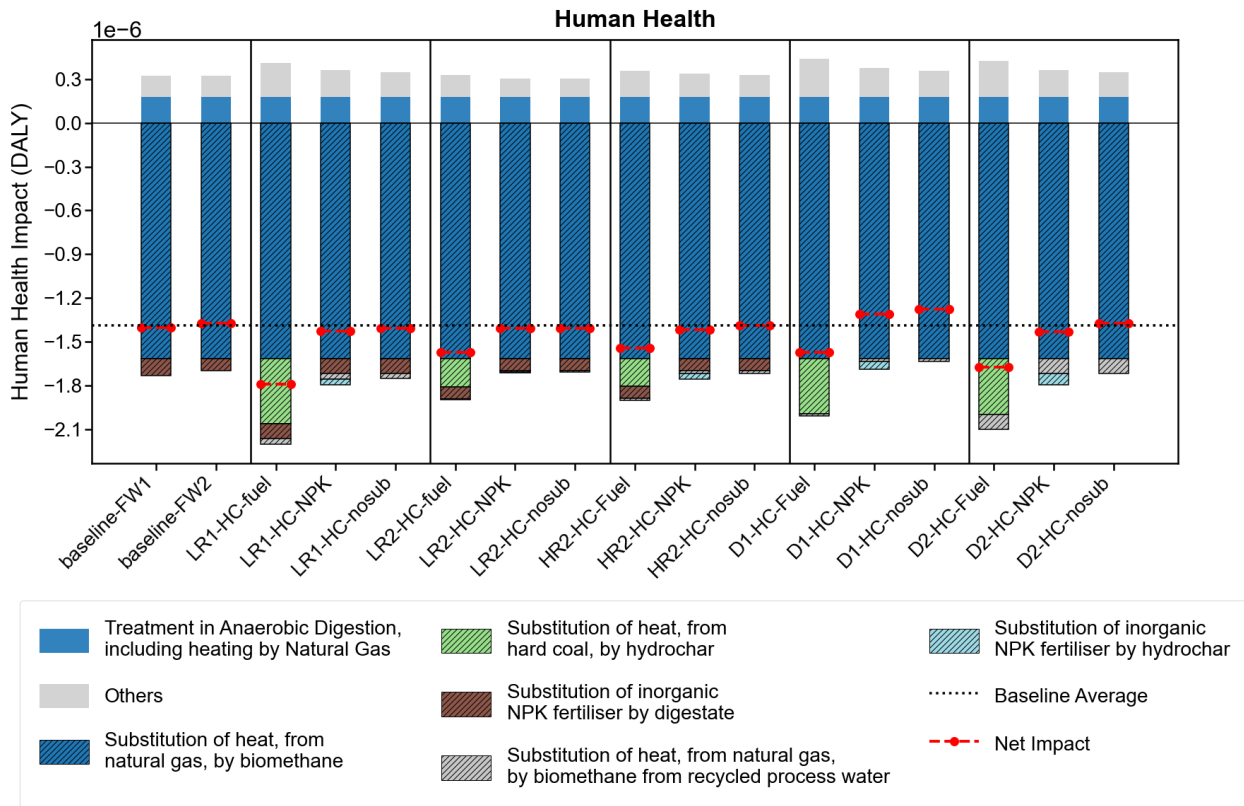


Figure S9: LCA results on the Total Human Health (HH) impact category for the 17 process configurations.

S7. Sensitivity Analysis for the LCA

The electricity mix was switched to an Ontario mix (denoted by “ON”) and the results show no significant difference between the Quebec configurations and the new ones on the CC impact category, albeit with a small difference between the configurations themselves coming from the greener overall electricity mix in Quebec. Nevertheless, this difference does not invalidate the conclusions drawn throughout the paper.

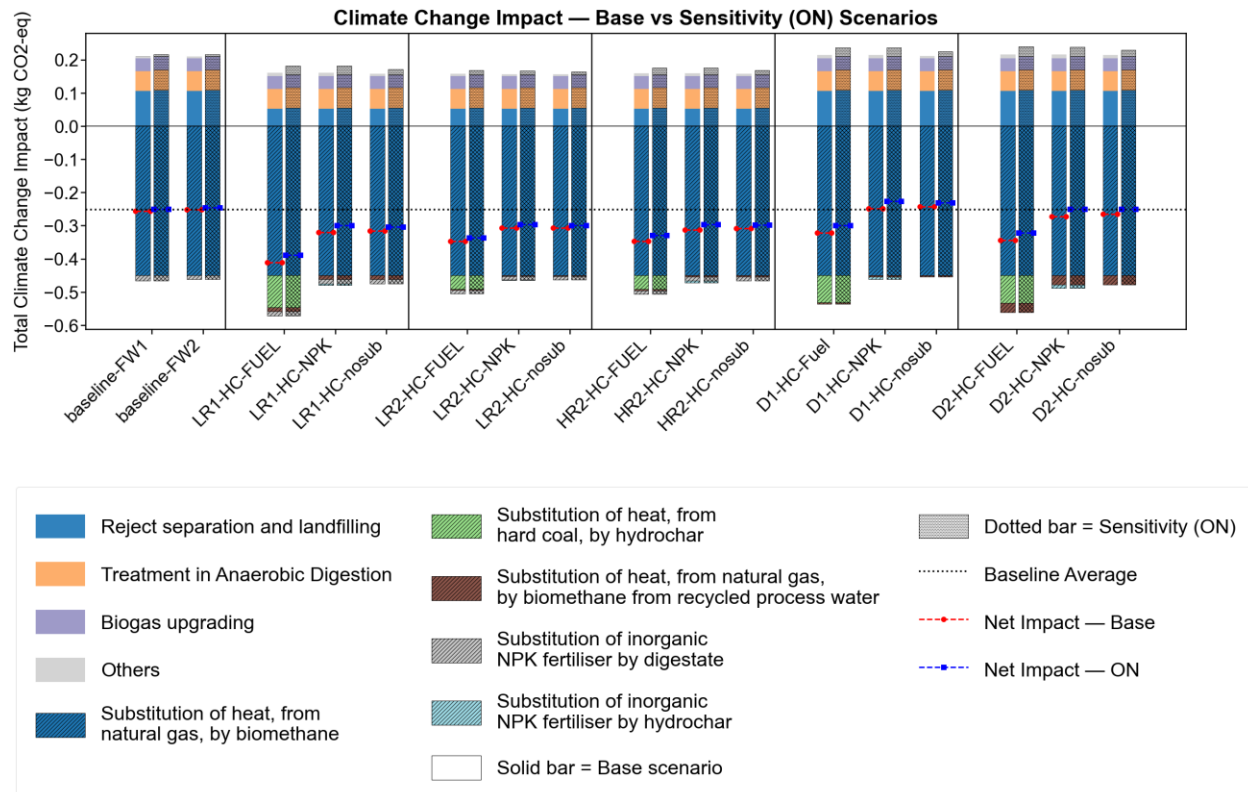


Figure S10: Effect of Electricity Mix (ON vs QC) on Climate Change Impact Across Configurations.

To further evaluate the robustness of the model, a sensitivity analysis was performed on the HTC solid load. The initial fixed value of 80% was adjusted to 75% and 70% across all configurations incorporating HTC. An exception was made for the D2 scenario; as the digestate was not dewatered prior to treatment, it was processed at its native moisture content. The results indicated negligible variations in the net climate change impacts, suggesting that the LCA outcomes are not sensitive to fluctuations in the HTC solid load within this range.

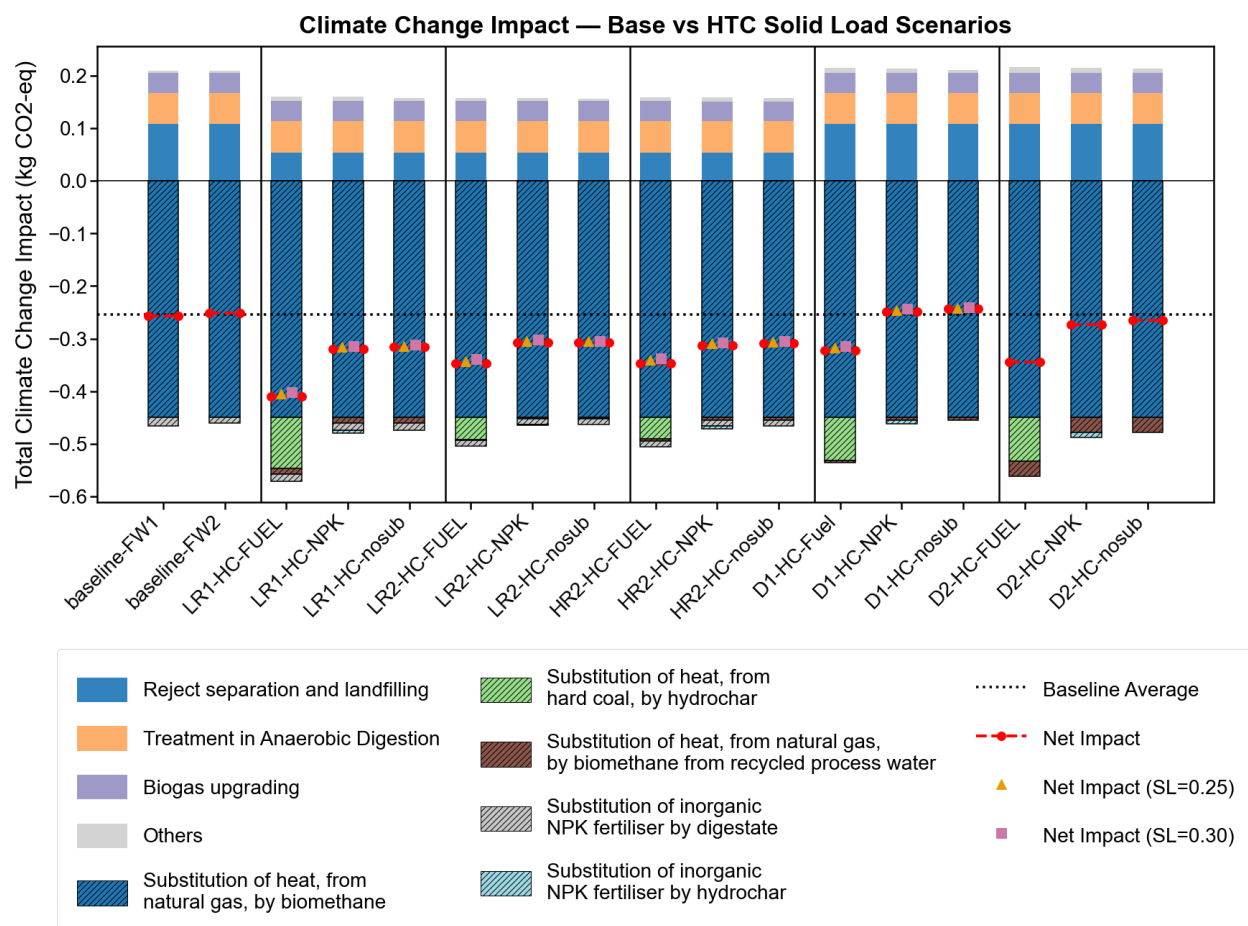


Figure S11: Effect of HTC solid load on Climate Change Impact Across Configurations.

References

- Marzban, N., Libra, J.A., Hosseini, S.H., Fischer, M.G., Rotter, V.S., 2022. Experimental evaluation and application of genetic programming to develop predictive correlations for hydrochar higher heating value and yield to optimize the energy content. *J. Environ. Chem. Eng.* 10, 108880. <https://doi.org/10.1016/j.jece.2022.108880>
- Mayer, F., Bhandari, R., Gäth, S.A., 2021. Life cycle assessment on the treatment of organic waste streams by anaerobic digestion, hydrothermal carbonization and incineration. *Waste Manag.* 130, 93–106. <https://doi.org/10.1016/j.wasman.2021.05.019>